

Journal Pre-proofs

Replacing PEG-surfactants in self-emulsifying drug delivery systems: Surfactants with polyhydroxy head groups for advanced cytosolic drug delivery

Julian David Friedl, Arne Matteo Jörgensen, Nguyet-Minh Nguyen Le, Christian Steinbring, Andreas Bernkop-Schnürch

PII: S0378-5173(22)00188-0
DOI: <https://doi.org/10.1016/j.ijpharm.2022.121633>
Reference: IJP 121633

To appear in: *International Journal of Pharmaceutics*

Received Date: 20 December 2021
Revised Date: 21 February 2022
Accepted Date: 28 February 2022

Please cite this article as: J. David Friedl, A. Matteo Jörgensen, N-M. Nguyen Le, C. Steinbring, A. Bernkop-Schnürch, Replacing PEG-surfactants in self-emulsifying drug delivery systems: Surfactants with polyhydroxy head groups for advanced cytosolic drug delivery, *International Journal of Pharmaceutics* (2022), doi: <https://doi.org/10.1016/j.ijpharm.2022.121633>

This is a PDF file of an article that has undergone enhancements after acceptance, such as the addition of a cover page and metadata, and formatting for readability, but it is not yet the definitive version of record. This version will undergo additional copyediting, typesetting and review before it is published in its final form, but we are providing this version to give early visibility of the article. Please note that, during the production process, errors may be discovered which could affect the content, and all legal disclaimers that apply to the journal pertain.

© 2022 Published by Elsevier B.V.



Replacing PEG-surfactants in self-emulsifying drug delivery systems: Surfactants with polyhydroxy head groups for advanced cytosolic drug delivery

Julian David Friedl¹, Arne Matteo Jörgensen¹, Nguyet-Minh Nguyen Le¹, Christian Steinbring¹,

Andreas Bernkop-Schnürch^{1*}

¹ *Department of Pharmaceutical Technology, University of Innsbruck, Institute of Pharmacy, Center for Chemistry and Biomedicine, 6020 Innsbruck, Austria*

*Corresponding author

Department of Pharmaceutical Technology, University of Innsbruck, Institute of Pharmacy, Center for Chemistry and Biomedicine, 6020 Innsbruck, Austria

Tel.: +43 512 507 58 600

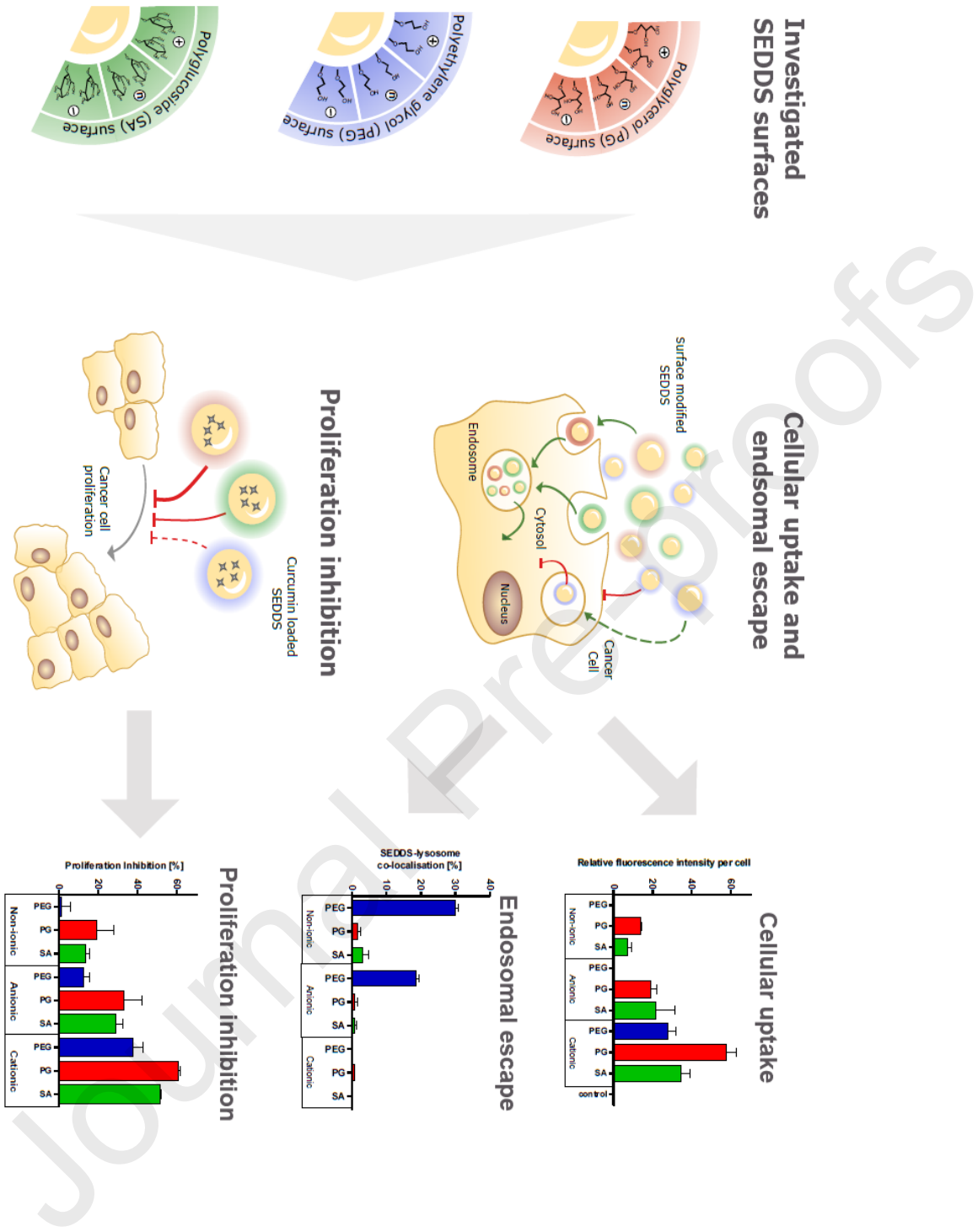
Email: Andreas.Bernkop@uibk.ac.at

The authors whose names are listed immediately above certify that they have no affiliations with or involvement in any organization or entity with any financial interest or non-financial interest in the subject matter or materials discussed in this manuscript. All authors have no *conflicts of interest to declare*.

Replacing PEG-surfactants in self-emulsifying drug delivery systems: surfactants with polyhydroxy head groups for advanced cytosolic drug delivery

The authors whose names are listed immediately above certify that they have no affiliations with or involvement in any organization or entity with any financial interest or non-financial interest in the subject matter or materials discussed in this manuscript. All authors have no *conflicts of interest to declare*.

Graphical Abstract



Abstract

Aim: Evaluation of different polyhydroxy surfaces in SEDDS to overcome the limitations associated with conventional polyethylene glycol (PEG)-based SEDDS surfaces for intracellular drug delivery.

Methods: Anionic, cationic and non-ionic polyglycerol- (PG-) and alkylpolyglucoside- (APG-) surfactant based SEDDS were developed and compared to conventional PEG-SEDDS. Particular emphasis was placed on the impact of SEDDS surface decoration on size and zeta potential, drug loading and protective effect, mucus diffusion, SEDDS-cell interaction and intracellular delivery of the model drug curcumin.

Results: After self-emulsification, SEDDS droplets sizes were within the range of 35-190 nm. SEDDS formulated with high amounts of long PEG-chain surfactants (> 10 monomers) a charge-shielding effect was observed. Replacing PEG-surfactants with PG- and an APG-surfactant did not detrimentally affect SEDDS self-emulsification, payloads or the protection of incorporated curcumin towards oxidation. PG- and APG-SEDDS bearing multiple hydroxy functions on the surface demonstrated mucus permeation comparable to PEG-SEDDS. Steric hinderance and charge-shielding of PEG-SEDDS surface substantially reduced cellular uptake up to 50-fold and impeded endosomal escape, yielding in a 20-fold higher association of PEG-SEDDS with lysosomes. In contrast, polyhydroxy-surfaces on SEDDS promoted pronounced cellular internalisation and no lysosomal co-localisation was observed. This improved uptake resulted in an over 3-fold higher inhibition of tumor cell proliferation after cytosolic curcumin delivery.

Conclusion: The replacement of PEG-surfactants by surfactants with polyhydroxy head groups in SEDDS is a promising approach to overcome the limitations for intracellular drug delivery associated with conventional PEGylated SEDDS surfaces.

Key words: PEG-free, polyhydroxy, surface modification, self-emulsifying drug delivery system (SEDDS), intracellular drug delivery, polyglycerol, saccharide

1. Introduction

Since decades surface functionalization with polyethylene glycol (PEG) is widely accepted as gold standard for polymeric [1], inorganic [2] and lipid-based NC [3, 4]. Among those lipid-based nanocarriers self-emulsifying drug delivery systems (SEDDS) are considered a promising platform for the mucosal delivery of small drugs as well as macromolecules. In case of SEDDS the oil droplet surface, consist of lipids conjugated to a PEG moiety as hydrophilic head group [5-7]. Such PEG-based surfactants and co-surfactants have become a prerequisite promoting the self-emulsification process of SEDDS in the gastro-intestinal tract (GIT) [7, 8]. To enable spontaneous dispersion in nano-sized o/w emulsions upon contact with water an extensive reduction of surface tension and interfacial energy is required to achieve a net zero or even negative free energy of the system [9]. Therefore, non-ionic PEG-surfactants such as polysorbates or PEGylated glycerides with HLB values >13 and long PEG head groups (> 10 monomers) in concentrations of more than 30-60% are used. When emulsified the PEG head groups assemble at the water/oil interface on the droplet surface, facing into the aqueous phase. Hence the surfactant head groups resemble the “face” of SEDDS and are predominantly determining the surface interaction with the GIT environment. Multiple advantages reported for SEDDS such as high colloidal stability, high mucus penetrating properties, cargo protection against degradation or enhancement of epithelial permeation are presumably attributed to their PEGylated surface [10]. For various other PEGylated NC the therefore required steric protection and chemical inertness to proteins such as mucins, degradative enzymes or membrane proteins is reported to be accompanied by substantial shortcomings for cellular uptake and endosomal escape, limiting the intracellular delivery of drugs [11, 12]. For SEDDS, so far this so called “PEG-dilemma” remained nearly unexplored. While recent research to improve the interaction of SEDDS with target cells has focused on cationic lipids, active

targeting moieties, cell-penetrating peptides or charge-converting surfaces [10, 13, 14], less attention was paid to the SEDDS surface and to find alternatives to PEG-surfactants. However, just recently, we elucidated the crucial role of PEG surfactants in the interaction between SEDDS and cells when, for the first time, polyglycerol-based (PG) surfactants were identified being capable to completely substitute PEG-surfactants for the development of SEDDS. By replacing long PEG chain (> 10 monomers) surfactants in SEDDS with polyglycerol (PG) based surfactant bearing short but highly hydrophilic PG (<6 monomers) head a reduced charge-shielding effect of the incorporated cationic lipids and subsequently an enhanced cellular uptake and intracellular displacement was observed [15]. Yet, it is still unknown whether these results are solely attributable to mitigated charge shielding by shorter PG chains, or whether the difference in head group chemistry might have affected SEDDS-cell interactions. Considering literature reports showing that polyhydroxy surfaces on NC can provide mucoinertness on the one hand [16] and superior cellular interaction over PEG-surfaces on the other [17], we hypothesized that the polyhydroxy head group of PG surfactants might have contributed to the results of the preceding study [15]. In this follow-up study, we aimed to verify this hypothesis by investigating another PEG-surfactant alternative bearing a short but very hydrophilic polyhydroxy head group. Hence, for the first time, an alkylpolyglucoside (APG) surfactant comprising a saccharide head group was assessed for the development of SEDDS (SA-SEDDS) with polyhydroxy surface. The different SEDDS surfaces illustrated in Figure 1 were compared for their cellular uptake, intracellular distribution and endosomal escape. Moreover, the impact of SEDDS surfaces on key parameters for drug delivery such as self-emulsification, drug incorporation and protection, mucus diffusion and pharmacological response were examined to evaluate the potential of polyhydroxy surface decorations as alternative to conventional PEG-SEDDS.

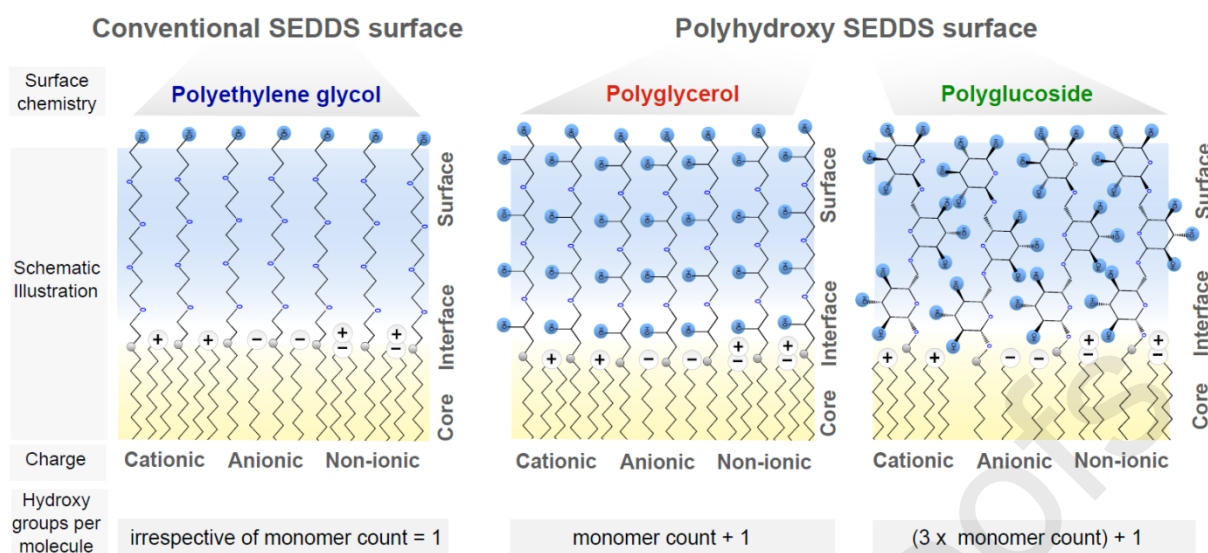


Figure 1. Schematic illustration of investigated SEDDS surfaces. Amphiphilic lipids such as mono- or diglycerides, which are presumably present at the emulsion interface, or oil components in the lipid core were omitted to simplify the graphical illustration.

2. Materials

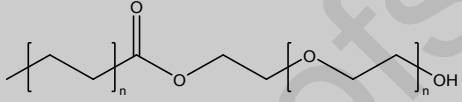
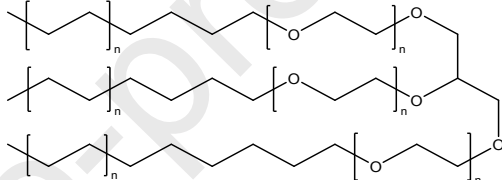
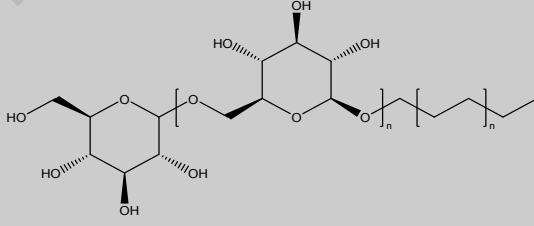
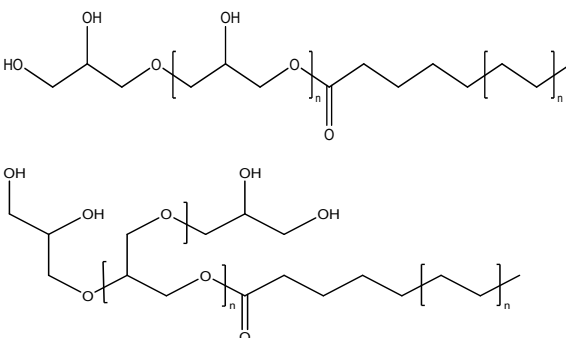
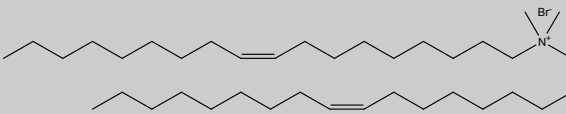
Capmul MCM C8 (glyceryl monocaprylate, G8MD) and Captex 355 (glyceryl tricaprinate, MCT) were donated by Abitec (Columbus, USA). Labrasol (PEG8- caprylic/capric glycerides, PEG8-glycerides), Peceol (Glyceryl monooleate, GMO), Gelucire 44/14 (Lauroyl PEG-32 glycerides, LPEG32G) and Gelucire 48/16 (PEG32-stearate) were a gift from Gattefosse (Lyon, France). Curcumin (from *Curcuma longa*, content >65%), Kolliphor RH40 (PEG40- hydrogenated castor oil, PEG40HCO), Kolliphor EL (PEG35-castor oil, PEG35CO), benzyl alcohol (BA), ethanol (EtOH), glycerol 85%, dimethylsulfoxide (DMSO), dioleoyldimethylammonium bromide (DODAB), sulforhodamine B, oleic acid and ethyl oleate were supplied by Sigma-Aldrich (Vienna, Austria). Tegosoft PC41 (PG4-caprate) and Tegosolve 90 (PG6-caprylate/PG4-caprate, PG4/6C) were a gift from Evonik (Hamburg, Germany). Natragem SP140 NP (PG-4 laurate/sebacate and PG-6 caprylate/caprinate, PG4LS/PG6CC) and Multitrope 1620 (alkylpolyglucoside, APG) were donated by Croda (Nettetal, Germany). Lumogen Red (LR) and Lumogen Orange (LO) were supplied by Kremer Pigmente (Aichstetten, Germany). Lipoid S 100 (soy phosphatidylcholine, PC) was obtained by Lipoid (Ludwigshafen, Germany). Fasted state simulated intestinal fluid (FasSIF) was purchased by Biorelevant (London, United Kingdom).

3. Methods

3.1. Preparation, characterization and stability of PEG-, PG- & SA-SEDDS

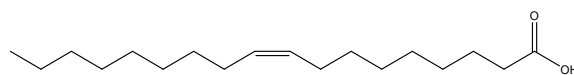
In a preliminary study various polyglycerol- (PG) and saccharide-based surfactants were examined for their self-emulsifying properties and compared to PEG-surfactants. The surfactants listed in Table 1 were chosen for the formulation of anionic, cationic and non-ionic SEDDS.

Table 1. List of surfactants investigated in this study sorted by their hydrophilic head group, surfactant class and hydrophilic-lipophilic balance (HLB) and chemical structure. Saturation and hydroxy functions of fatty acid residues were omitted to simplify the graphical illustration. An indeterminate number of repetitive chemical units of either lipophilic alkyl- or polymer chain is represented by "n".

Head group	Surfactant class	Investigated surfactants	HLB	Monomer Count	Chemical structure
Polyethylene glycol (PEG)	PEG fatty acid ester	PEG32-stearate	12	32	
	PEG glyceride esters	LPEG32G	11	32	
		PEG35CO	12-14	35	
		PEG40HCO	14-16	40	
	PEG8-glycerides	12	8		
Carbohydrate (SA)	Alkyl poly glucoside	C8-C10 polysaccharide	13	1-3	
Polyglycerol (PG)	PG fatty acid monoester	PG4-caprate	14	4	
		PG4/6C	15	4-6	
		PG4LS/PG6CC	14	4-6	
Charge inducing lipids	Cationic lipid	Dioleyl dimethyl ammonium bromide			

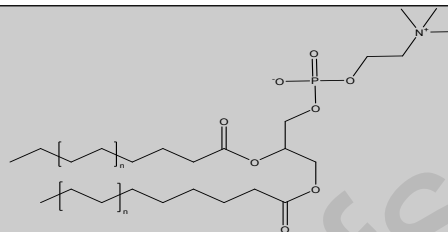
Anionic
lipid

Oleic Acid



Zwitter-
ionic
lipid

Phosphatidyl-
choline



Oils, surfactants and co-solvents were mixed in the ratios given in Table 2 using a batch size of 200 μ L. In order to prepare SEDDS with a positive surface charge the cationic lipid dioleoyldimethylammonium bromide (DODAB), a cationic lipid, was introduced into the oil phase while oleic acid was used to provide a negative charge under physiological pH. Final pre-concentrates were vigorously mixed at 40°C and 1200 rpm on a thermomixer (Eppendorf, Hamburg, Germany) to obtain homogenous isotropic mixtures. Pre-concentrate instability in terms of phase separation or component precipitation were evaluated after centrifugation for 15 min at 10.000 rpm (Eppendorf Minispin, Hamburg, Germany).

Table 2: Composition of SEDDS preconcentrates in %. The "*" indicates whether the listed compounds are classified as main surfactant "**", oil "***" or co-surfactant/co-solvent "*****".

Non-ionic	PEG	Ethyloleate**	GMO	BA***	PC in EtOH*** (300 mg/ml)	LPEG32G*	PEG32-stearate*
		50%	10%	10%	5%	10%	15%
	PG	Ethyloleate**	GMO	BA***	PC in EtOH (300 mg/ml)	PG4-caprate*	
		15%	10%	10%	5%	60%	
	SA	Ethyloleate**	GMO	BA***	PC in EtOH*** (300 mg/ml)	APG*	
		40%	10%	10%	5%	35%	
Anionic	PEG	GMO**	BA***	Oleic acid**	G8MD**	MCT**	PEG40HCO*
		10%	10%	2%	8%	40%	30%
	PG	GMO**	BA***	Oleic acid**	G8MD**	PG4/6C*	
		5%	5%	2%	8%	80%	
	SA	GMO**	BA***	Oleic acid**	G8MD**	APG*	
		10%	25%	2%	8%	55%	
Cationic	PEG	GMO**	PC in EtOH*** (300 mg/ml)	BA***	DODAB in MCT (120 mg/ml)**	MCT**	PEG35CO* PEG8-glycerides*
		15%	5%	20%	25%	25%	5%
	PG	GMO**	PC in EtOH*** (300 mg/ml)	BA***	DODAB in MCT (120 mg/ml)**	PG4LS PG6CC*	PG4-caprate*
		15%	5%	20%	25%	25%	10%
	SA	GMO**	PC in EtOH*** (300 mg/ml)	BA***	DODAB in MCT (120 mg/ml)**	APG*	
		15%	5%	20%	25%	35%	

Droplet size and PDI were investigated after dispersing and slightly agitating SEDDS preconcentrates in a 1:100 (v/v) ratio in demineralized water utilizing dynamic light scattering technique (Malvern Zetasizer ZSP, Worcestershire, UK). Zeta potential was measured in triplicate using a palladium electrode equipped dip cell (Malvern Universal Dip Cell, Worcestershire, UK). Emulsified SEDDS were further subjected to centrifugation at 5000 rpm for 10 min to test their thermodynamic stability. In addition, a stability test under in-vivo simulating conditions was performed. Therefore, SEDDS preconcentrates were emulsified in a final concentration of 1% (v/v) in fasted simulated intestinal fluid (FasSIF) incubated for 4 h and subsequently analysed for changes in their droplet size, PDI and zeta potential. FasSIF medium with a pH of 6.5 containing mixtures of bile salts and phospholipids was prepared according to the preparation protocol given by the supplier.

3.2. Determination of preconcentrate viscosity

Using a rheometer (Haake Mars Rheometer, 379-0200, Thermo Electron GmbH, Karlsruhe, Germany) with a plate-plate fixture (PP35 Ti, D = 35 mm) and a plate distance of 0.5 mm, flow curves depicting shear-dependent viscosity of SEDDS preconcentrates were acquired. After incubation at 20°C, 700 µL of each sample was placed on the plate and rheological measurements with linear shear rates ranging between 0 and 10 s⁻¹ were performed. The mean viscosity was calculated from 50 points within a shear rate range of 5-10 s⁻¹ to take the shear rate-dependent changes in viscosities into consideration. Each given value is a mean of three viscosity measurements.

3.3. Evaluation of self-emulsification properties

Self-emulsification properties of PEG-, PG- and SA-SEDDS were assessed in three different experiments. First, self-emulsification time was determined utilizing the USP dissolution apparatus type II (Erweka DT 600, Heusenstamm, Germany). 1 ml of concentrate was pipetted into 900 mL of demineralized water at $37\text{ }^{\circ}\text{C} \pm 0.5\text{ }^{\circ}\text{C}$ and gentle stirring at 50 rpm was provided by a standard stainless-steel paddle imitating intestinal agitation. The time for complete emulsification was evaluated visually. To improve the visualisation, SEDDS concentrate was labelled with the lipophilic fluorescence marker Lumogen Orange (LO) in a concentration of 0.2 mg/mL. Complete and homogenous dispersion of the fluorescence marker in the vessel served as experimental end point.

Second, pre-emulsified SEDDS were diluted with increasing amounts of demineralized water from 1% up to 0.0001% [v/v] to compare the robustness against dilution of PEG-SEDDS by adapting a method previously described by Agrawal et al. [14]. After incubation for 10 min at $37\text{ }^{\circ}\text{C}$ and under gentle agitation at 500 rpm utilizing a thermomixer (Eppendorf, Hamburg, Germany), the size of oily droplets was analysed at each dilution step. An increase in size above 300 nm and PDI higher 0.3, indicating a non-monodisperse distribution of the droplets size, were chosen as experimental endpoints.

The minimal dilution concentration necessary for self-emulsification was determined as third indicator for the self-emulsification properties of PEG-, PG- & SA-SEDDS by utilizing a method earlier described by Rohrer et al. [18]. In brief, starting from the 1:100 dilution with demineralized water, the amount of concentrate was gradually increased (v/v) and the amount of water was decreased accordingly. The emulsions formed were analysed for particle size and PDI at $37\text{ }^{\circ}\text{C}$ using the Zetasizer. After centrifugation at 10.000 rpm for 10 min the

formulations were examined for physical changes such as precipitation or phase separation. The highest concentration still resulting in oil droplets with sizes <300 nm and PDI < 0.3 was identified as the minimal dilution concentration.

3.4. Log D of curcumin (SEDDS_{preconcentrate}/water)

For determination of Log D (SEDDS_{preconcentrate}/water) the maximum saturation concentration of curcumin (C_{max}) was measured in PEG-, PG- and SA-SEDDS preconcentrates on the one hand as well as in demineralized water on the other hand. To determine C_{max} of curcumin in preconcentrates and in demineralized water, 50 mg of drug were dispersed in either 1000 μ L of the preconcentrates or demineralized water. The drug- preconcentrate and drug-water suspensions were stirred at 1000 rpm for 24 h at 25 °C in a thermomixer followed by a centrifugation at 13.000 rpm for 10 min (MiniSpin[®], Eppendorf Austria GmbH). Finally, 100 μ L of supernatant were mixed with 900 μ L of ethanol and analysed for curcumin absorbance at a wavelength of 425 nm using UV-VIS spectrometry. Based on a linear calibration curve ($r^2=0.999$) of curcumin in ethanol the concentration of curcumin in the supernatants were calculated. Log D was calculated using the following equation:

$$\text{Log } D \left(\frac{\text{SEDDS}}{\text{water}} \right) = \log \left(\frac{c(\text{curcumin}) \text{ in SEDDS}}{c(\text{curcumin}) \text{ in water}} \right)$$

3.4.1. Curcumin degradation

In vitro oxidation of curcumin was performed to investigate the protective effect of SEDDS against oxidative degradation of curcumin. In presence of H_2O_2 , peroxidases oxidize curcumin to a bicyclopentadione consequently leading to a loss of its chromophoric system [19]. For the in vitro degradation a slightly adopted method by Gordon et al. was applied [20]. Curcumin

was incorporated in SEDDS preconcentrate at a concentration of 2 mg/mL and a 1% (m/m) SEDDS dispersion in phosphate buffer saline (PBS) pH 7.4 was prepared, resulting in a final concentration of 20 µg/mL curcumin. In a 96 well plate set-up, 180 µL of this dispersion were combined with 10 µL of 1 U/mL horse radish peroxidase (HRP) solution and 10 µL of 1 mM H₂O₂. Directly after mixing, the absorbance of curcumin was measured at 425 nm in intervals of 20 seconds for 10 min. Curcumin-loaded SEDDS without HRP/H₂O₂ mixture served as 100% value while curcumin-loaded SEDDS with H₂O₂ but without enzyme represented the negative control and unloaded SEDDS were subtracted as blank values. The degradation curves were compared to the oxidative degradation of unprotected curcumin dissolved in PBS.

3.5. Mucus permeation studies

Prior to the assay, intestinal mucus was collected from freshly excised porcine intestine and further purified following the standard protocol developed in our research group [21]. The time between the slaughter and freezing of mucus was kept as short as possible to preserve its macro-rheological properties. The mucus permeation of PEG-, PG- and SA-SEDDS was investigated using via two well-established experiments [22, 23]. First, SEDDS mucus penetration depth was examined by the rotating cylinder using a slightly modified test set-up previously described by Pereira de Sousa et al. [23]. Silicon tubes of 5 cm length and 4 mm diameter were filled with mucus and sealed at one end. SEDDS preconcentrates were labelled with Lumogen orange (LO) in a concentration of 1 mg/mL. Preconcentrates of PEG-, PG- and SA-SEDDS were controlled for comparable fluorescence intensities after dispersion in 25 mM HEPES buffer pH 7.4 in a concentration of 2% (v/v). For each formulation 50 µL of SEDDS emulsified in water (1% v/v) were gently pipetted on top of the mucus at the remaining open

end of the tube. Subsequently the tubes were sealed completely and incubated at 37°C under horizontal rotation (50 rpm) for 12 h. Afterwards, the tubes were frozen at -80°C and cut into slices of 2 mm length. To extract the lipophilic fluorescence marker from the mucus each slice was incubated with 150 µL of DMSO for 24 h under light protection. After an additional hour of ultra-sonication the samples were centrifuged for 5 min at 13.400 rpm. 100 µL of supernatant were withdrawn and analysed at a $\lambda_{\text{ex}} = 485 \text{ nm}$ and $\lambda_{\text{em}} = 530 \text{ nm}$ using a spectrophotometer (Tecan; Salzburg, Austria). HEPES buffer served as blank and was subtracted from the sample fluorescence intensity.

In a second study, SEDDS permeation through a defined mucus layer into a donor chamber was investigated by the trans-well system previously introduced by Leichner et al. [22]. Therefore, 50 µL of purified mucus corresponding to a mass of 55 mg was dropped onto the insert membrane of a 24-well plate (ThinCert cell culture insert for 24-well plates, transparent polyethylene terephthalate membrane, pore diameter: 3.0 µm, Greiner-Bio One, Austria). After shaking the plate for 2 min with 1800 rpm on a thermomixer (Eppendorf, Hamburg, Germany) a homogenous mucus layer with a thickness of 1.6 mm and a defined surface area of 33.6 mm² was obtained. The donor chamber was filled with 300 µL with LO labelled SEDDS (1 mg/mL) dispersed in 25 mM HEPES buffer in a concentration of 2% (v/v). The acceptor chamber was filled with 600 µL of prewarmed HEPES buffer. During the incubation at 37°C and 50 rpm in an orbital shaking incubator the plate was sealed to prevent water evaporation. Each hour up to 4 h, 100 µL of sample were collected from the acceptor chamber to analyse the fluorescence intensity as described above. The equivalent volume was replaced with preheated HEPES buffer. In order to take membrane absorption effects into account the amount of permeated dye of a 2% (v/v) SEDDS dispersion through the insert membrane lacking the mucus layer served as 100% control.

3.6. Cell viability - resazurin assay

The cytotoxic potential of PEG-, PG- and SA-SEDDS was evaluated by resazurin reduction assay [24]. A Caco-2 cell line was selected as it closely resembles the small intestinal epithelia as site of absorption [25]. Cells were seeded in a density of 5×10^5 Caco-2 cells/mL in a 96-well plate and incubated in minimal essential medium (MEM) for 48 h at 95% humidity and 37°C in an atmosphere of 5% CO₂ to obtain a monolayer. MEM containing 10% (v/v) heat inactivated fetal calf serum (FCS) and penicillin/streptomycin solution (100 units in a concentration of 0.1 mg/L) was used as nutrition media.

Previous to the experiment SEDDS were dispersed in concentrations ranging from 2%- 0.01% (v/v) in iso-osmolar, sterile glucose-HEPES buffer at pH 7.4. Before addition of 100 µL of SEDDS formulation to the Caco-2 cell layer MEM was discarded. After 4 h of incubation at 37 °C the samples were removed and cells were washed twice to rinse of remaining SEDDS from the cell surface. Subsequently, 150 µL of a 0.1% (m/v) resazurin solution in white MEM (MEM lacking the indicator phenol red) were applied to each well followed by 2 h of incubation. After the reaction time 100 µL of supernatant were withdrawn and analysed at $\lambda_{\text{ex}} = 540$ nm and $\lambda_{\text{em}} = 590$ nm using a microplate reader (Tecan; Salzburg, Austria). As negative and positive control pure white MEM and Triton X-100 in concentration of 0.5% (m/v) were chosen.

3.7. Membrane interaction - hemolysis assay

The susceptibility of red blood cells (RBC) to membrane disruption followed by a release of hemoglobin is used to mimic the interaction of drugs or NC with biological membranes [26, 27]. RBC, kindly donated by Tirol Kliniken GmbH (Innsbruck, Austria), were diluted with sterile

iso-osmolar glucose-HEPES buffer pH 7.4 in a ratio of 1:100 (v/v). 0.5 mL of this erythrocyte dilution were added to an equal volume of SEDDS dispersed glucose-HEPES buffer pH 7.4. The resulting SEDDS concentration in the RBC-SEDDS mixture ranged from 0.5% - 0.00075% (v/v). The RBC-SEDDS mixtures were incubated in a thermomixer (Eppendorf, Hamburg, Germany) at 300 rpm and 37°C for 4 h. The mixture was subjected to centrifugation at 2350 rpm for 10 min and the supernatant containing the released hemoglobin from lysed erythrocytes was analysed by absorbance measurement at a wavelength of 415 nm (Tecan, Salzburg, Austria). Triton X-100 in a concentration of 0.5% (v/v) dissolved in the HEPES buffer served as 100% reference value of hemolysis (positive control) and iso-osmolar buffer containing RBC in equal concentrations served as negative control.

Hemolysis (%) was calculate by using the equation below:

$$\% \text{ Hemolysis} = \frac{Abs(T) - Abs(neg)}{Abs(pos) - Abs(neg)}$$

Where Abs (T) is absorbance of test sample, Abs (neg) is absorbance of the negative control and Abs (Pos) is absorbance of the positive control.

3.8. Cellular uptake studies

Flow cytometry (FC) analysis was used to determine the impact of SEDDS surface on cellular uptake. SEDDS were labelled with 0.1% (m/m) Lumogen RED (LR). To prevent falsified results by inhomogeneous fluorescence intensities in the different SEDDS preconcentrates, two emission wavelength scans (λ_{ex} 405nm & 488 nm; λ_{em} 450-800 nm) were recorded and compared prior to the experiment. LR labelled SEDDS preconcentrates were diluted in sterile glucose-HEPES buffer pH 7.4 to a final non-toxic concentration of 0.025 % (m/m). Caco-2 cells in a density of 5×10^4 cells/ mL were seeded in a 24 well plate (Greiner Bio-One, Germany)

and cultivated for 7 days in order to obtain a fully confluent monolayer. For cellular uptake the monolayer was incubated with 500 μL of labelled SEDDS for 4 h at 37°C. Subsequently, 200 μL of Accutase® were added to detach the cells followed by three washing steps with 500 μL of ice cooled 10 mM PBS pH 7.4. The amount of LR taken up by Caco-2 cells was analysed via flow cytometry (Attune NxT Flowcytometer, Thermofisher Scientific). Data were analyzed using a custom-written MatLab program (FCalyzer) utilizing a neuronal network (self-organizing map network) for autonomous cluster detection in the FSC-A/SSC-A and FSC-A/FSC-W space. Fluorescence intensity distribution data were represented using logicle display. The average concentration of LR-labelled SEDDS taken up per single cell is given as relative median fluorescence intensity values (RMFI). RMFI values were calculated using the following equation:

$$RMFI = \frac{MFI(sample)}{MFI(control)} - 1$$

where MFI = median fluorescence intensity. Based on this equation, the RMFI value of untreated Caco-2 cells is always 0. For each sample > 10000 cells were analysed and constant gating settings were applied.

3.9. Confocal microscopy study

In order to evaluate intracellular SEDDS distribution in Caco-2 cells confocal laser scanning microscopy (Leica TCS SP8) was conducted. Briefly, 8- well chamber slides (μ -slide, Ibidi) with density of 1×10^5 Caco-2 cells/well were prepared and incubated for 5 days until the cells reached 100% confluency. 300 μL of LR-labelled SEDDS, having been prepared as described in the FC section, were added to the monolayer and incubated for 4 h. Subsequently, Caco-2 monolayers were rinsed with pre-warmed 10 mM PBS pH 7.4 twice before applying Hoechst

33528 and LysoView 633. The cell nucleus was stained using Hoechst 33528 in a concentration of 1 $\mu\text{g}/\text{mL}$ for 8 min, whereas lysosomal staining was performed utilizing LysoView 633 in a concentration of 1 mg/mL for 30 min. All fluorescence images were recorded under equal confocal settings. Image postprocessing was performed utilizing the open source image processing and analysis platform ImageJ: the yz- and xz-projections were prepared from 5 xy-images of an image stack taken at 0.2 μm z-step length. Additionally, 100 XY-projections of a single image plane located at the middle of the cell were averaged in order to visualize the distribution pattern of PEG-, PG- and SA-SEDDS throughout the cytosol. To eliminate fluorescence bleed through between detection channels due to overlapping emission spectra, spectral inmixing was performed. In addition, 2D image filtering by using a Gaussian filter was applied.

In order to determine the intensity-distribution of each formulation across the Caco2-layer, a sliding window approach was used, written in MatLab. In short, the mean intensity distribution along the z-axis of the stack image data is determined using a volume of the size $W/a \times H/a \times z$, (tested for $a=1, 9, 36$). Within the volume, the cell-layer boundaries (top, bottom) were determined in a semiautomatic approach (based on the nucleus and SEDDS-intensity profile); the program suggests the cell-layer-boundaries to the user. Subsequently the user verifies the correct boundary position via the image data (using a maximums-projection of the chosen volume in y-direction). An average curve was calculated based on the volume-fraction curves for each sample.

3.10. Pharmacological activity - proliferation inhibition assay

The sulforhodamine B (SRB) assay as previously reported by Orellena et al. [28] was slightly adopted to examine the proliferation inhibition of curcumin loaded SEDDS. In brief, Caco-2

cells were seeded in a 96 well plate at a low cell density of 2×10^4 cells /mL and cultivated under equal conditions as described above. After 24 h of culturing, 100 μ L of SEDDS loaded with curcumin (5 mg/ml) emulsified in a concentration of 0.02% (v/v) in sterile glucose-HEPES buffer pH 7.4 were added to the colon carcinoma cells and incubated for 2 h. After incubation, SEDDS were withdrawn and the cells were gently washed with PBS and further cultivated with Red-MEM until wells containing the untreated control reached 100% confluency. Subsequently, 25 μ L of 50% (m/v) trichloric acid were added and the plate was kept at 4°C for 60 min to fix the cells. After fixation the plates were thoroughly rinsed with tap water and left overnight at room temperature (RT) to dry completely. To the dried cells 50 μ L of a 0.04% (m/v) SRB solution in 1% acetic acid was added and incubated for 60 min at RT. Another 4 washing steps with 1% acetic acid solution removed unbound dye. After a further drying step, 100 μ L of Tris base (10 mM) pH 10.5 were poured into the wells and shaken for 15 min at RT to dissolve SRB. The amount of SRB in supernatant was detected by absorbance measurement at a wavelength of 510 nm. Cells incubated with curcumin free SEDDS at equal concentration displayed the 100% growth control. Curcumin dissolved in HEPES buffer in the same concentration as in SEDDS served as reference. Growth inhibition was calculated as follows:

$$\% \text{ growth inhibition} = 100 - \left(\text{Absorbance} \frac{\text{sample}}{\text{control}} * 100 \right)$$

3.11. Statistical data analyses

Statistical data analysis was performed on GraphPad Prism (version 5.01) using the student *t*-test and the analysis of variance (ANOVA) followed by Bonferroni correction with $p < 0.05$ as the minimal level of significance. All values are expressed as means \pm SD.

4. Results and discussion

4.1. Evaluation of self-emulsifying properties

In a preliminary study various polyglycerol (PG-) and saccharide-based surfactants were screened for their use in self-emulsifying-systems. Due to their substantial hydrophilicity the miscibility with oils of most saccharide-based surfactants such as sucrose ester, rhamnolipids and alkylglucamides was poor. In contrast, alkylpolyglucoside- (APG-) surfactants demonstrated adequate miscibility and solubilisation of various oils in water by micelle formation (data not shown). Hence, an APG-surfactant was used for the preparation of SEDDS comprising a polyglucoside surface (SA-SEDDS). For preparation of PEG-, PG-, SA-SEDDS the different surfactants were mixed with oils and cosolvents as listed in Table 2. A set-up of three experiments was conducted to compare the self-emulsifying properties of PG- and SA-SEDDS with conventional PEGylated SEDDS.

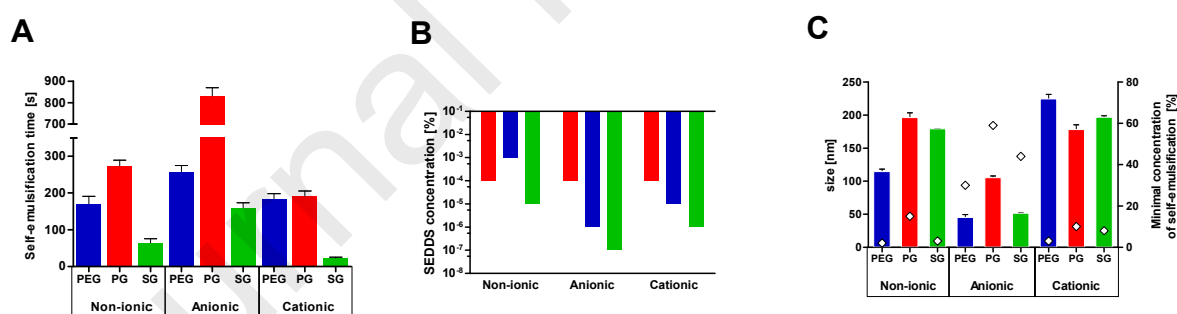


Figure 2. **A** Self-emulsification time, **B** robustness against dilution and **C** minimal dilution concentration [v/v in %] required for self-emulsification (diamonds) and the respective droplet size of non-ionic, anionic and cationic PEG- (blue), PG-(red), SA- (green) SEDDS emulsified in demineralised water. Data are shown as mean \pm SD (n=3)

As illustrated in Figure 2A, the self-emulsification was impacted by the SEDDS oil core composition and the different surfactants types. Using higher amounts of co-solvent (e.g

cationic group) or low viscosity oil components in SEDDS pre-concentrates (e.g. non-ionic group) lowered the viscosity of pre-concentrates (supportive Figure 1). In addition, a correlation between pre-concentrate viscosity and surfactant type was found, as viscosity in each group followed the trend PEG- < SA- < PG-surfactant. As a low pre-concentrate viscosity eases interfacial surface shearing and water penetration the pre-concentrate self-emulsification is accelerated. Hence, higher viscosity of PG-SEDDS thus explains the correspondingly longer self-emulsification times. Moreover, PG-SEDDS demonstrated pre-concentrate gelation upon contact with water, additionally contributing to the significantly higher emulsification time compared to PEG- and SA-SEDDS. As gelation was already reported in formulations with high PEG-surfactant concentrations likely the high S/O-ratios and the capability of PG-surfactants to form intra- and intermolecular H-bonds leads to pre-concentrate gelation. Although, the latter also applies for SEDDS pre-concentrates based on APG-surfactants, SA-SEDDS emulsified the fastest in each group and no pre-concentrate gelation was noticed. As depicted in Figure 2B, adequate stability towards high dilutions was observed for all SEDDS formulations confirming the potential of PG- and APG-surfactants to stabilize oil droplets within in-vivo relevant dilutions. In addition, the results displayed in Figure 2C suggest that the hydrophilicity of SEDDS oil core is a major factor reducing the minimum amount of dispersion medium required for self-emulsification. On average, PG- and APG-based formulations showed adequate self-emulsification at 2- to 5-fold lower dilutions compared to PEG-SEDDS, rendering them promising alternatives for target sites with reduced amounts of dispersion media such as the ocular or nasal epithelium.

4.2. Characterization and stability of PEG-, PG- & SA-SEDDS in simulated intestinal fluid

The droplet size, PDI and zeta potential of SEDDS are displayed in Table 3. The deviations in droplet size within each group were with $< \Delta 20$ nm for non-ionic, $< \Delta 12$ nm for cationic and $< \Delta 30$ nm for anionic SEDDS comparatively small. As highlighted in various studies, the NC size is a well-explored parameter not only affecting the extent of NC uptake, but also determining the predominant uptake pathways. NC with around 50 nm were observed to be internalized more efficiently than smaller particles (about 15-30 nm) or larger particles (about 70-240 nm). For particles with a size of 120-150 nm, internalization occurs mainly by clathrin- or caveolin-mediated endocytosis, whereas larger particles rely on micro- and macropinocytosis pathways [29]. Consequently, a comparable droplet size of the SEDDS formulations is required to eliminate these contributing factors and correlate the cellular uptake to the variations in the surface properties of SEDDS. As displayed in Table 4 across all formulations PEG-SEDDS exhibited the lowest surfactant to oil (S/O) ratio in each group. On average, significantly lower concentrations of PEG-surfactants were required compared to PG- and the APG-surfactant to emulsify the same amount of oil and form emulsions of comparable droplet size. This is in line with the reported modest ability of PG- and saccharide based surfactants to reduce the interfacial tension compared to polysorbate and PEG-esters surfactants [30].

Table 3: Size, PDI and zeta potential of SEDDS emulsified 1% [v/v] in demineralized water.

	Surfactant type	Size [nm]	PDI	Zetapotential [mV]
Non-ionic	PEG	158.6 ±0.8	0.20 ±0.02	-0.5 ± 0.8
	PG	187.8 ±1.6	0.10 ±0.01	-7.5 ±0.3
	APG	149.3 ±8.1	0.07 ±0.01	-8.5 ±0.3
Anionic	PEG	38.5 ±4.6	0.05 ±0.01	-6.73 ±0.2
	PG	96.8 ±1.5	0.13 ±0.02	-19.8 ±0.7
	APG	73.4 ±1.5	0.19 ±0.01	-19.3 ±0.5
Cationic	PEG	179.3 ±6.6	0.19 ±0.01	53.1 ±1.4
	PG	177.4 ±4.0	0.17 ±0.02	58.3 ±0.6
	APG	158.7 ±4.1	0.17 ±0.02	61.5 ±0.5

The zeta potential deviations are with $< \Delta 7.5$ mV for anionic, $< \Delta 4.5$ mV for cationic and 4.5 non-ionic SEDDS minor, however, PEG-SEDDS possessed the closest to zero zeta potential in each group. Particularly when high amounts of long-PEG chain surfactants were used, for instance in the anionic group a pronounced charge-shielding effect in comparison to PG- and SA-SEDDS was noticed. In a previous study, we explored this charge-shielding for cationic SEDDS for the first time and found a charge decline of $\Delta 5.9$ mV when 10% long-chain PEG-surfactant and $\Delta 11.6$ mV when 40% was incorporated [15]. This charge-shielding effect can be attributed to the non-ionic hydrated polymer surface of conferred by PEG-surfactants which was also reported in various studies for liposomes and other lipid NC [15, 31].

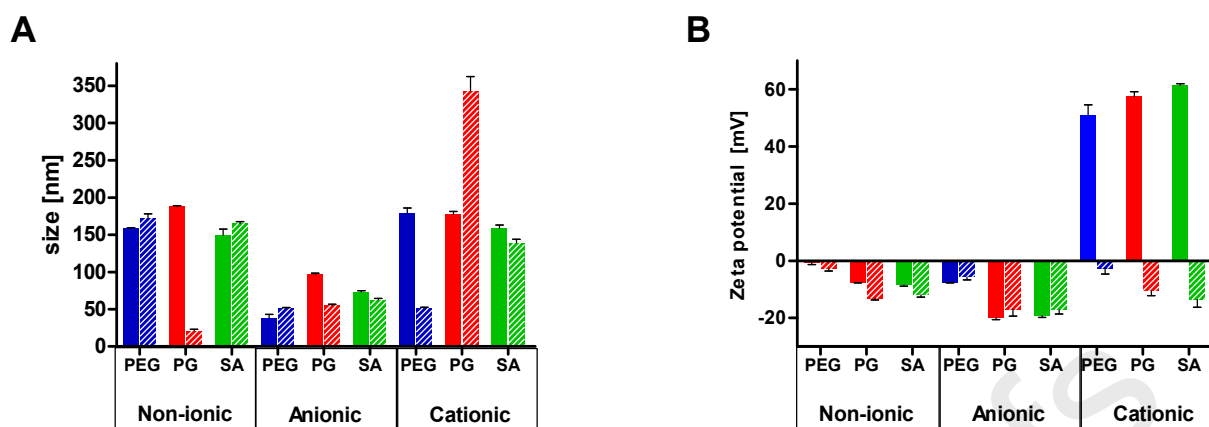


Figure 3. **A** Droplet size and **B** zeta potential of non-ionic, anionic and cationic PEG- (blue), PG- (red), APG- (green) SEDDS emulsified in concentration of 1 % (v/v) after 4 h incubation at 37°C in demineralized water (filled bars) and fasted-state simulated intestinal fluid (lined bars). Data are shown as mean \pm SD (n=3).

As shown in Figure 3A, the changes in droplet size after 4 h incubation of SEDDS in FasSIF were within Δ 12-20 nm comparable for most formulation. In particular PG-SEDDS were susceptible to size alteration due to interactions of bile salts or lipids in the simulated intestinal fluid, resulting in changes ranging from Δ 40-165 nm. But also cationic PEG-SEDDS showed a drastic size decline. The more pronounced changes were observed for the zeta potential displayed in Figure 3B. Zeta potential reduction was detected for all non-ionic and cationic SEDDS after incubation in FasSIF. In each group, the presence of bile salts and lipids led to decreased zeta potential with the group of cationic SEDDS being the most pronounced. This tendency was also observed by Lupu et al. [32]. Moreover, for cationic SA- and PG-SEDDS zeta potential reduction was with Δ 75.0 and Δ 67.8 mV higher compared to PEG-SEDDS (Δ 53.4 mV), which is in line with previous findings on PG-SEDDS incubated with bile salts [15]. PEGylation of NC was proven to stabilize the NC within the GIT environment [1, 33]. Our data suggest that bile salts or digestion lipids have a more pronounced impact on PG- and APG-surfactants based SEDDS

compared to PEG-SEDDS. However, up to now the consequences of a pronounced or minor bile salt interaction for the in-vivo performance of SEDDS have not been resolved yet.

4.3. Payload, Log D and oxidative stability of curcumin loaded in SEDDS

Drug loading and stability towards oxidative degradation of curcumin as lipophilic model drug incorporated in PG- and SA-SEDDS was evaluated and compared to conventional PEG-SEDDS. As presented in Table 4, the payload of curcumin in SEDDS was in the range of 0.86-3.02 % (m/v) for all investigated formulations. Thus, assuming a 2% (v/v) dilution, the water solubility of curcumin was improved by at least 57 up to 200-fold after incorporation in SEDDS.

Table 4: Surfactant to Oil (S/O) -ratio, Log D [SEDDS preconcentrate/H₂O], max payload of curcumin in SEDDS.

	Surfactant type	S/O-ratio	Log D (SEDDS/H ₂ O)	Max. payload curcumin [%]
Non-ionic	PEG	0.42	3.55 ±0.03	2.82±0.05
	PG	2.40	3.28 ±0.03.	1.42 ±0.03
	APG	0.70	3.15 ±0.03	1.05 ±0.02
Anionic	PEG	0.52	3.06 ±0.02	0.86 ±0.01
	PG	6.15	3.61 ±0.03	3.02 ±0.06
	APG	3.06	3.40 ±0.02	1.85 ±0.02
Cationic	PEG	0.25	3.36 ±0.02	1.70 ±0.02
	PG	2.34	3.52 ±0.02	2.44 ±0.03
	APG	2.34	3.47 ±0.03	2.19 ±0.04

The varying curcumin payloads in SEDDS preconcentrates are a result of an interplay of several factors such as different c_{\max} of curcumin in SEDDS components, varying S/O-ratios of

formulations and co-solubility phenomena between the different surfactants and other SEDDS components.

For SEDDS, the Log D between SEDDS preconcentrate and the dispersion media (Log D (SEDDS/water)) was established as reliable parameter to predict the distribution of lipophilic drugs from the oil into the aqueous continuous phase [34]. The experimental Log D values (Table 4) of curcumin in the investigated preconcentrates ranged from 3.06 to 3.61. The higher the log D value and the smaller the release media volume the lower the amount of curcumin released from the oil droplets. Based on a dilution factor of 1:50, the in-vivo assumed percentage of immediately released curcumin would remain between 1.3 % and 4.4 % for the investigated SEDDS formulations. Since oxidative degradation of curcumin represents a major limitation for its in-vivo efficacy [19], the protective properties of SEDDS against oxidation of their payload were investigated. As evident from Figure 4, incorporation of the BCS 4 drug curcumin into SEDDS oil core significantly reduced the model drugs oxidation.

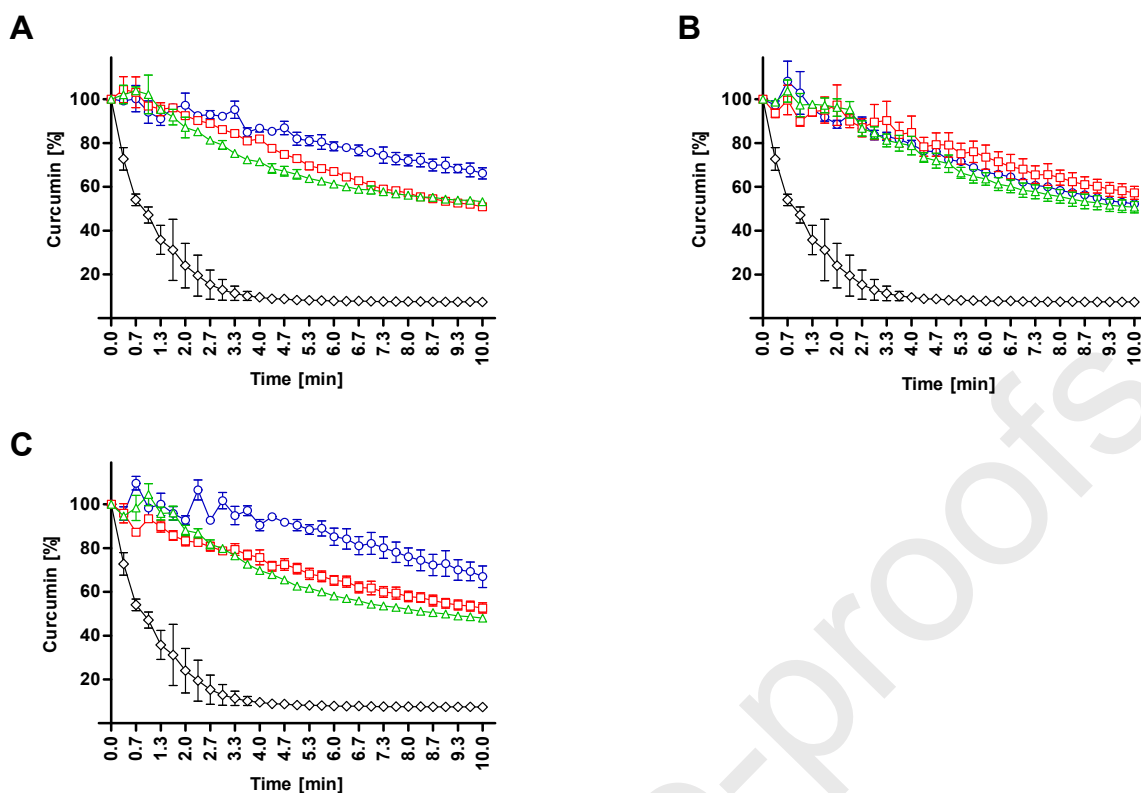


Figure 4. Oxidative degradation of curcumin incorporated in **A** non-ionic, **B** anionic and **C** cationic PEG- (blue circles), PG- (red squares), SA- (green triangles) SEDDS emulsified in concentration of 1 % (v/v) in phosphate buffer saline pH 7.4. Pure curcumin solution (black diamonds) in phosphate buffer saline. Data are shown as mean \pm SD (n=3)

While unformulated curcumin was nearly completely oxidized within 120 seconds, more than 50% of the original payload was recovered for all formulations after the entire assay duration. Seo et al. demonstrated the relevance of drug protection with respect to highly oxidative biological target sites. The cytotoxic effect of free doxorubicin, in contrast to doxorubicin formulated in nanotubes, was reported to be completely suppressed in the presence of a peroxidase in the microenvironment of melanoma and lung carcinoma cells [35]. Although no trend for either surfactant type or surface charge of SEDDS was apparent, the observed oxidative protection after incorporation in SEDDS could enhance the therapeutic potential of curcumin in oxidative environments.

4.4. Mucus penetration and permeation

The mucus diffusion depth was assessed by rotating cylinder method and the permeation of SEDDS across a defined mucus layer in a transwell set-up as illustrated in Figure 5AB and in supportive Figure 2. In both set-ups, it could be confirmed that the surface charge has significant influence on mucus interaction. The already well-documented mucus permeation trend of anionic > non-ionic > cationic surface charge is related to the electrostatic repulsion of anionic and the attraction of cationic NC with anionic mucus substructures promoting mucus permeability or entrapment, respectively [36].

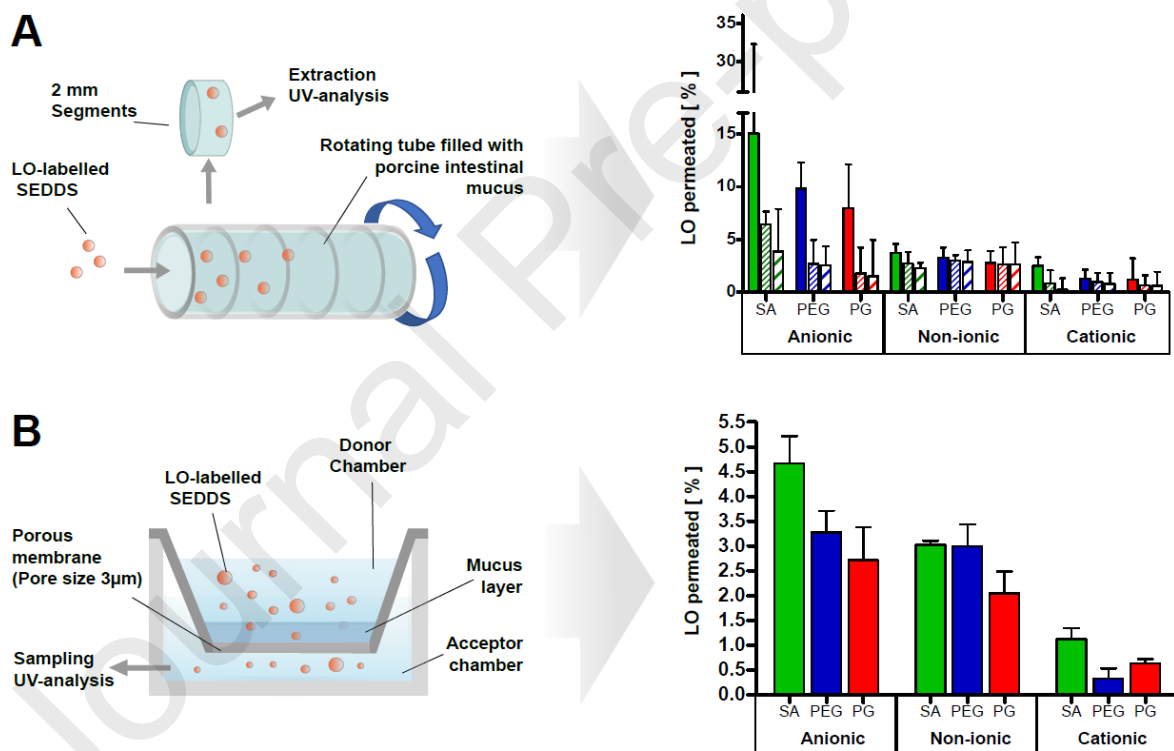


Figure 5. **A** Schematic illustration of the rotating tube set-up and the resulting diffusion depth detected for non-ionic, anionic and cationic PEG- (blue), PG- (red) and SA- (green) SEDDS in first mucus segment (filled bars), second mucus segment (thin lined bars) and third mucus segment (thick lined bars). **B** Schematic illustration of the transwell set-up and the resulting total amount of anionic, non-ionic and cationic PEG (blue), PG (red) and SA- (green) SEDDS permeated across a defined, freshly excised porcine mucus layer after 4 hours.

Regarding the influence of surface decoration, SA- and PG- SEDDS showed comparable mucus permeation to common PEGylated SEDDS surfaces in both experiments. The results obtained for SEDDS with polyglucoside surface in the anionic group indicate a slightly enhanced mucus penetration compared to PEG-SEDDS and PG-SEDDS. Most likely, this finding can be explained by the comparatively higher zeta potential of PEG-SEDDS, caused by pronounced charge-shielding effect of PEGylated vs the polyglucoside surface of SA-SEDDS. However, as non-ionic saccharide coatings are known to confer rather mucoadhesive properties by H-bond pairing or surface entanglement with the mucus mesh [37-39] these findings were unexpected.

Up to now, mucus interaction studies of SEDDS bearing non-PEGylated surfaces are missing since PEG-surfactants are widely recognized as prerequisite for their formulation. But also, for other NC PEGylation is considered state of the art for creating mucus penetrating NC [38, 40]. However, lately also polyhydroxy function bearing polymers were considered as potential muco-inert coatings [16] and in particular 2-hydroxypropyl methacrylate (HPMA) is applied for muco-inert surface coatings [41, 42]. Cui et al. reported a direct correlation between an increase in the surface hydrophilicity of a PLGA-NC coated with HPMA and a decrease in mucus interaction, along with an increase in the apparent permeability coefficient through the mucus layer [43]. On the one hand hydroxy functions in the head group of PG- and the APG-surfactant display extensive water affinity thus formation of a hydrated shell at the surface similar to PEG-coatings is possible. On the other hand the shorter head group chain length could prevent the entanglement of surface structures with the mucus mesh as reported for high molecular weight PEG-surfaces [44].

4.5. Cell viability

As depicted in Figure 6 at concentrations above 0.025% (v/v) each formulation exposed a cell viability $\geq 80\%$ and can be considered as non-toxic to Caco-2 cells.

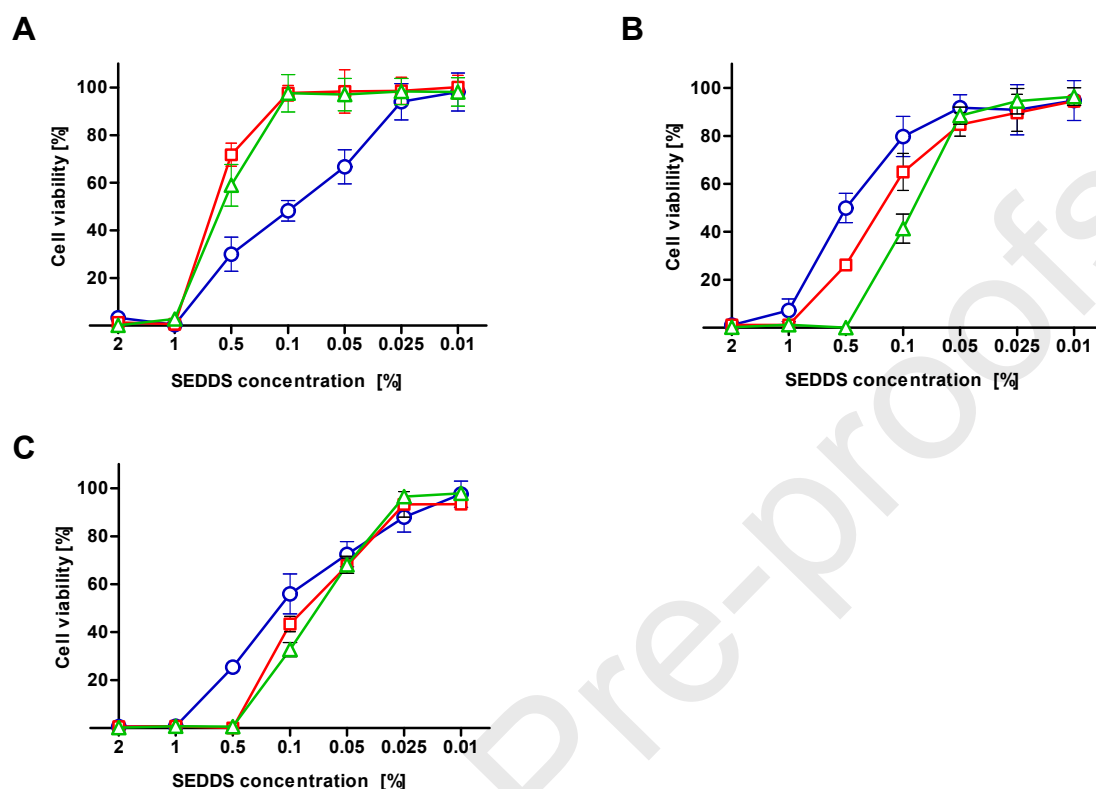


Figure 6. Cellular viability [%] of Caco-2 cells after 4 h incubation with **A** non-ionic, **B** anionic and **C** cationic PEG- (blue circles), PG- (red squares), SA- (green triangles) SEDDS at indicated concentrations. Triton X 100 served as positive control and red MEM as negative control. Data are shown as mean \pm SD (n=3)

The IC_{50} values listed in Table 5 indicate the highest cytotoxic potential for the group of cationic SEDDS, followed by the group of anionic and non-ionic group, which is in agreement with various other studies in the field demonstrating an increased interaction of cationic charged NC with anionic membrane proteins promoting NC binding and depolarization of cellular membranes [45, 46]. However, non-ionic PEG-SEDDS presented an exception to this tendency. Data on the cytotoxicity of unformulated PEG32-fatty acid ester on Caco-2 cells by Sachs-Barrable et al. [47] demonstrated identical toxicity profile compared to non-ionic PEG-SEDDS. Assuming that for most o/w emulsion published (75%) the added surfactant remains

unadsorbed in the continuous phase [48] the intrinsic toxicity of the surfactant can dominate the cytotoxicity of the formulation. Besides surfactant toxicity also the charge-shielding effect of dense PEG-surface influenced cell viability. The IC_{50} of anionic PEG-SEDDS was 2- to 3.7-fold higher compared with the corresponding PG- and SA-SEDDS, indicating that the inert PEG-surface impedes the interaction between charged lipids and cells.

Table 5: IC_{50} and HC_{50} values of SEDDS in [%] v/v.

	Surfactant type	IC_{50}	HC_{50}
Non-ionic	PEG	0.14 ± 0.02	0.008 ± 0.000
	PG	0.56 ± 0.25	0.066 ± 0.001
	APG	0.53 ± 0.03	0.044 ± 0.002
Anionic	PEG	0.34 ± 0.04	0.019 ± 0.003
	PG	0.17 ± 0.03	0.007 ± 0.001
	APG	0.09 ± 0.01	0.007 ± 0.007
Cationic	PEG	0.12 ± 0.01	0.004 ± 0.001
	PG	0.08 ± 0.01	0.005 ± 0.001
	APG	0.07 ± 0.03	0.003 ± 0.000

Membrane interaction studied via hemolysis assay on red blood cells (RBC) presented in supportive Figure 3, confirmed these findings. While the hemolytic potential of SEDDS was more impacted by SEDDS surface charge than by different surface decoration (IC_{50} values in Table 5) again the latter is not negligible especially taking charge-shielding and steric protection of high concentration of long-PEG chain surface (e.g. anionic PEG-SEDDS) into account.

4.6. Cellular uptake and intracellular distribution of PEG-, PG-, SA-SEDDS

The impact of SEDDS surface charge and decoration on their uptake by Caco-2 cells was evaluated by flow cytometry and confocal microscopic imaging. While Figure 7A depicts the average amount of LO signal per cell in terms of RFMI values, Figure 7B represents the percentage of Caco-2 cells exposing a fluorescent signal. Aside the surface charge, the SEDDS surface decoration significantly influenced the cellular internalisation. The formation of a dense PEGylated surface by PEG-32 fatty acid ester in non-ionic PEG-SEDDS reduced their unspecific uptake drastically as evidenced by the uptake curves plotted in the supportive Figure 4, RFMI values (Figure 7A) and percentages of cellular uptake (Figure 7B). This is in line with reports by Wehrung et al. describing a sound reduction in cellular uptake of NC corresponding to increasing amounts of PEG-32 fatty acid esters on the NC surface [49]. Moreover, their data on PEG-NC biodistribution emphasize the so-called PEG-dilemma. The enhanced in-vivo circulation time or biodistribution of PEGylated NC, goes hand in hand with sacrificing the NC-cell interaction at the target site as a trade-off [3, 11]. A significantly reduced SEDDS-cell interaction resulting in over 75-fold higher RFMI could also be observed when comparing anionic PEG-SEDDS with their positively charged counterpart. This profound difference cannot only be accounted to the increased uptake of positively over negatively charged SEDDS surfaces, but also to a more pronounced charge-shielding effect resulting from a 6-fold higher amount of long PEG-chain surfactants in anionic compared to cationic PEG-SEDDS. In an earlier study we could correlate the charge-shielding effect of a dense PEG-surface to the diminished uptake of cationic PEG-SEDDS [15]. A step wise reduction of polysorbate 80 in cationic SEDDS, in exchange with PG-4- and PG-6-surfactants resulted in a higher cellular uptake of SEDDS, as a result of the decreased charge-shielding effect of smaller PG-surfactant head groups. Also, in this study the cationic PG-SEDDS exhibited a twofold

higher intracellular accumulation than PEG-SEDDS. However, as also the cellular uptake of non-ionic and anionic PG-SEDDS was exceeding those of their PEGylated counterparts a superior internalisation by PG-surfaces independent of their charge or their reduced charge-shielding effects was confirmed.

Notably, also SA-SEDDS outperformed PEGylated SEDDS in each group with respect to the number of fluorescence signals per single cell and to the percentage of cells which had been taken up. Consequently, a correlation between the increased uptake of SEDDS, and the multiple hydroxyl functions on the surface is conceivable.

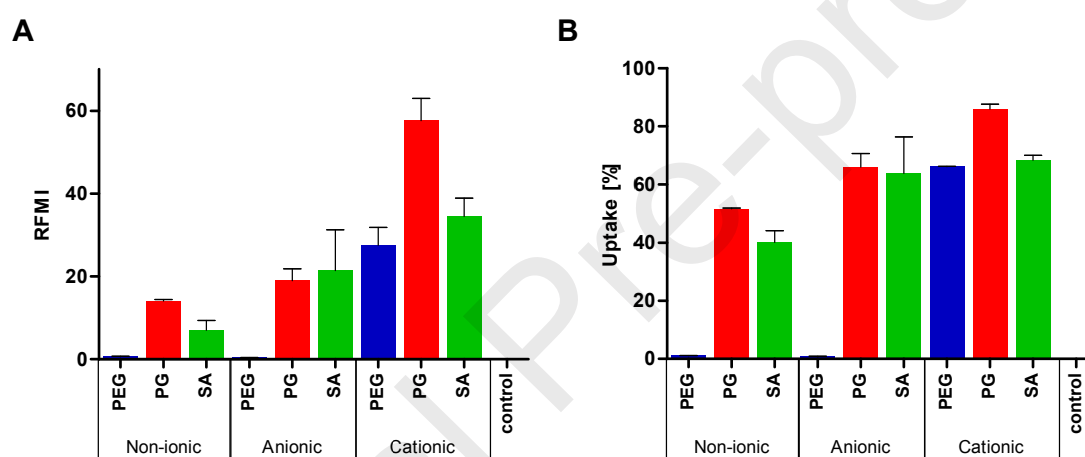


Figure 7. **A** Average amount of fluorescence signals per single cell displayed as relative mean fluorescence intensity values (RFMI) after uptake of non-ionic, anionic and cationic PEG- (blue), PG- (red), SA- (green)-SEDDS after 4 h incubation determined by flow cytometry. **B** Average amount of Caco-2 cells [%] displaying a fluorescence signal equivalent to the cell uptake of non-ionic, anionic and cationic PEG- (blue), PG- (red), SA- (green)-SEDDS after 4 h determined by flow cytometry. Caco-2 cells without SEDDS served as control. Data are shown as mean of 3 experiments \pm SD

The confocal images in Figure 8 visually verify the uptake data retrieved by FACS analysis. Image analysis confirm increased cellular uptake of PG- and SA-SEDDS over PEGylated SEDDS in all investigated formulations. Three-dimensional imaging and image analysis in supportive Figure 5 indicate a relatively unrestricted distribution of SEDDS, particularly for PEG-surfactant based formulations, throughout the cytosol, with accumulation tendencies towards the cell

centre. Thus, a perinuclear distribution of SEDDS involving a vesicular transport pathway and the Golgi apparatus might be assumed. For positively charged SEDDS, a shift of the distribution curves peaks toward higher z-intercepts was observed, suggesting a deeper penetration in the cell layer closer to the cell bottom.

Since conventional nanoemulsions with PEG-surfaces are frequently reported to be up taken via clathrin-mediated endocytosis [50, 51], endosomal escape is a prerequisite for effective cytosolic drug delivery to avoid drug degradation in the late endosome or lysosomes. As illustrated in Figure 9, non-ionic and anionic PEG-SEDDS exhibited high co-localisation with fluorescent-labelled lysosomes, corroborating above mentioned charge-shielding effect of inert PEG-surfaces impeding SEDDS-membrane interaction. On the contrary, reduced charge-shielding of only 5% long PEG chain surfactant and the incorporation of the cationic charged lipid DODAB prevented the endosomal entrapment, as no lysosomal co-localisation was detected for cationic PEG-SEDDS.

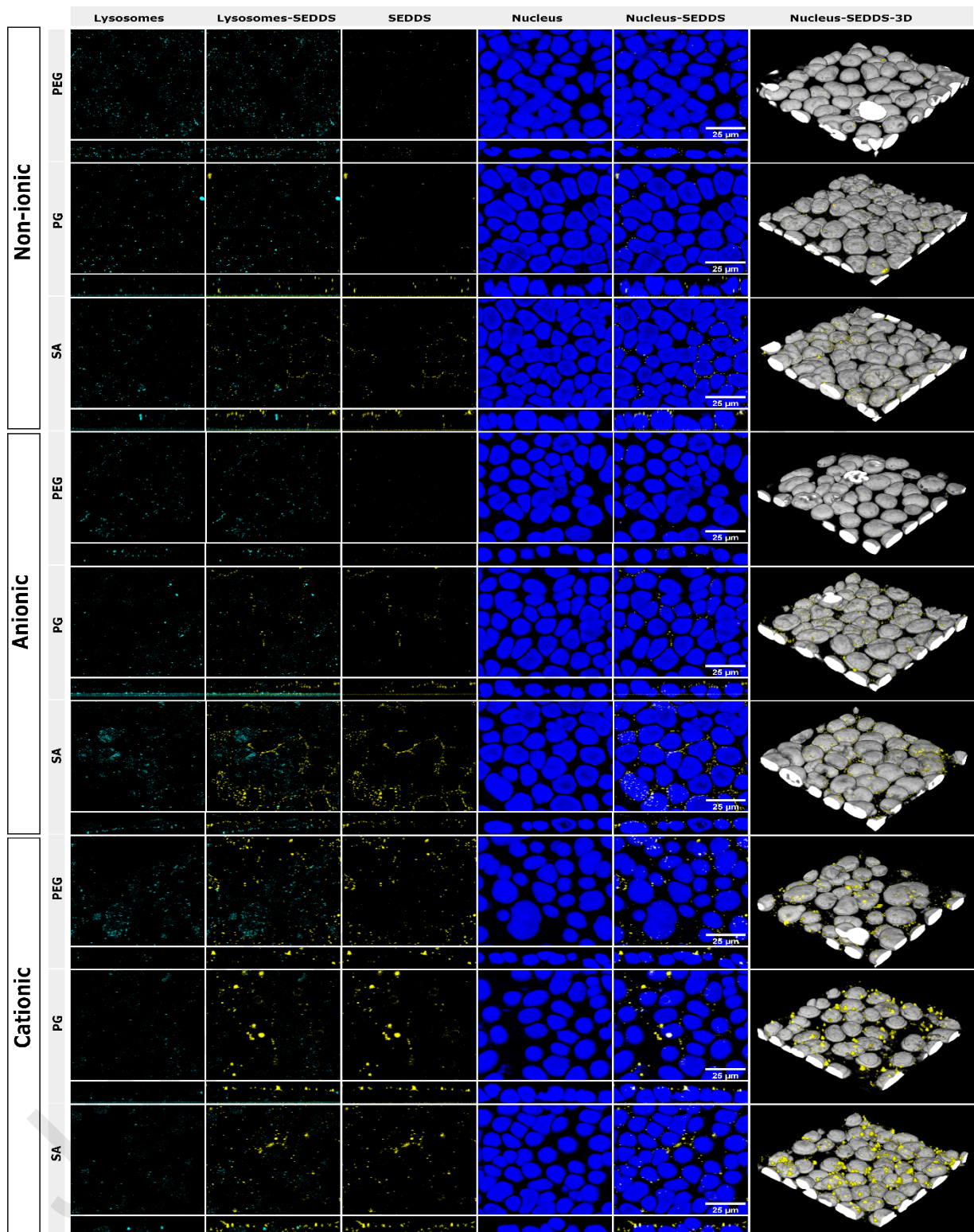


Figure 8. Cellular uptake of non-ionic, anionic and cationic PEG- (blue), PG- (red), SA- (green)-SEDDS by Caco-2 cells visualized by confocal microscopy. From left to right lysosomes (turquoise), up taken SEDDS (yellow), a merged image of lysosomes and SEDDS (turquoise/yellow), the cell nucleus (blue), a merged 2-D image SEDDS/nucleus (yellow/blue) and a merged 3-D image SEDDS/nucleus (yellow/grey) are displayed. Lumogen red was incorporated in SEDDS as fluorescence marker. Nuclei were stained with Hoechst 33528 and lysosomes with Lysoview 633.

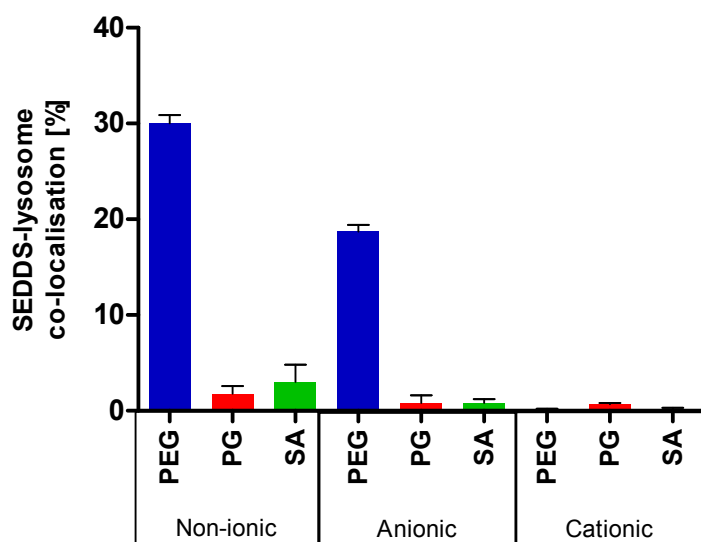


Figure 9. Percentage of SEDDS co-localized with lysosomes after uptake of non-ionic, anionic and cationic PEG- (blue), PG- (red), SA- (green)-SEDSS using confocal image analysis. Data are shown as mean \pm SD (n=3)

Intriguingly, neither charged nor uncharged surface PG- and SA-SEDSS were co-located lysosomes, assuming a fusion and subsequent escape of polyhydroxy decorated SEDSS from the endosome or an uptake mechanism potentially omitting lysosomal fusion. In a literature review hydroxylated NC were found to be increasingly internalised by lipid rafts via a caveolae-mediated transport mechanism [52]. Recently, also Edlich et al. observed an clathrin-independent uptake for nanogels on polyglycerol basis [53]. Moreover, for SEDSS based on APG-surfactants the glucose moiety bearing SEDSS surface could trigger receptor-mediated uptake by the GLUT-receptor family. Glucose-modified NC surfaces were explored for targeting cancer cells based on their over-expression of GLUT-receptors, but also lipid raft-mediated uptake was reported glycosylated NC [54-56]. A clathrin-independent uptake of polyhydroxy decorated SEDSS on the one hand might explain the increased uptake in particular of anionic and non-ionic PG- and SA-SEDSS on the other hand the absence of lysosomal co-localisation after internalisation.

4.7. Pharmacological activity - Proliferation inhibition

Based on the results shown in Figure 10, the potential of SEDDS to deliver BCS 4 drugs to cancer cells and elicit a physiological response was found to be affected by the surface charge on the one hand and by the different surface decorations to proliferation inhibition in the order PG > SA > PEG on the other hand.

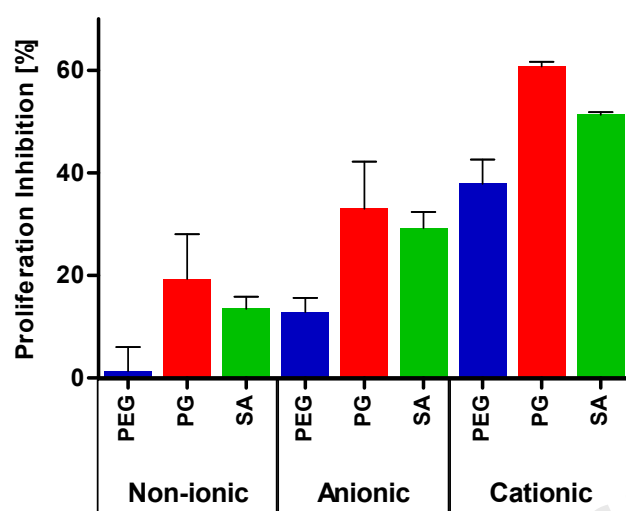


Figure 10. Proliferation inhibition of Caco-2 cells after 2 h incubation with non-ionic, anionic and cationic PEG- (blue), PG- (red), SA- (green) SEDDS. Cells incubated with SEDDS in equal concentrations without curcumin served as 100% growth control. Data are shown as mean \pm SD (n=3)

With a final concentration of only 1 μ g/mL curcumin loaded PG-SEDDS caused pronounced proliferation inhibition in concentrations at least 3 times lower compared to literature values of unformulated curcumin [57, 58]. Worth mentioning is the intracellular mechanism of action of curcumin. Via interaction with several cytosolic proteins, curcumin induces cell cycle arrest in G2/M phase and apoptosis [57], necessitating cytosolic release of the drug to trigger a pharmacological response. Based on the proliferation inhibition and confocal imaging data, polyhydroxy surfactants with small but highly hydrophilic head groups bear high potential to increased SEDDS-cell interaction and cytosolic delivery of drugs. Moreover, combining and precisely balancing PEG -and hydroxy-moieties on SEDDS surfaces was reported being a promising strategy to overcome PEG associated drawbacks without sacrificing the benefits.

Lund et al. observed a synergistic effect of a 50/50 modified surface bearing PEG-NH₂ and glucose increased cellular uptake 18-fold compared to surfaces solely modified with PEG-NH₂ or glucose [59]. Thus, using different surfactants types might not only synergistically advance the intracellular drug delivery but also expand the horizon for surface modifications, active targeting or stimuli responsive SEDDS.

5. Conclusion

In this work, we systematically investigated the role of PEG-surfactants and surfactants bearing polyhydroxy head groups in SEDDS with the objective to resolve the PEG-dilemma of conventional SEDDS and to improve intracellular drug delivery. The replacement of PEG-surfactants in SEDDS formulation by PG- and an APG-surfactant did not detrimentally affect SEDDS self-emulsification properties, payload, or protective effect towards oxidation of the formulated model drug curcumin. Moreover, PG- and APG-based SEDDS showed similar mucus-permeating properties as their PEGylated counterparts. The steric hindrance and the charge-shielding effect of an inert PEG surface drastically hindered the internalization and endosomal escape of non-ionic and anionic PEG-SEDDS and merely positively charged PEG-SEDDS showed significant cellular uptake and low lysosomal co-localization. In contrast, polyhydroxy decorated SEDDS demonstrated irrespective their surface charge a superior cellular uptake, endosomal escape and consequently a higher inhibition of tumor cell proliferation after cytosolic delivery of curcumin. Hence, a correlation between increased cellular uptake and the multiple hydroxyl functions on the SEDDS surface is conceivable. While no PEGylated formulation was able to simultaneously provide high mucus permeability, cellular uptake and endosomal escape, negatively charged polyhydroxy surfaces on SEDDS successfully combined all these features. Thus, replacing PEG-surfactants by surfactants with a polyhydroxy head group represents a causal approach to overcome the PEG dilemma for mucosal delivery of drugs acting on intracellular targets.

Acknowledgements

The authors want to sincerely thank Magdalena Höller for her assistance and the inspiring discussions. This work was supported by a doctoral scholarship for the promotion of young researchers at the Leopold-Franzens-University Innsbruck.

References

- [1] J.M. Rabanel, P. Hildgen, X. Banquy, Assessment of PEG on polymeric particles surface, a key step in drug carrier translation, *J Control Release* 185 (2014) 71-87.
- [2] J. Conde, J.T. Dias, V. Grazú, M. Moros, P.V. Baptista, J.M. de la Fuente, Revisiting 30 years of biofunctionalization and surface chemistry of inorganic nanoparticles for nanomedicine, *Front Chem* 2 (2014) 48-48.
- [3] M.L. Immordino, F. Dosio, L. Cattell, Stealth liposomes: review of the basic science, rationale, and clinical applications, existing and potential, *Int J Nanomedicine* 1(3) (2006) 297-315.
- [4] D. Santonocito, M.G. Sarpietro, C. Carbone, A. Panico, A. Campisi, E.A. Siciliano, G. Sposito, F. Castelli, C. Puglia, Curcumin Containing PEGylated Solid Lipid Nanoparticles for Systemic Administration: A Preliminary Study, *Molecules* 25(13) (2020).
- [5] S. Savić, S. Tamburić, M.M. Savić, From conventional towards new – natural surfactants in drug delivery systems design: current status and perspectives, *Expert Opinion on Drug Delivery* 7(3) (2010) 353-369.
- [6] J. Jiao, Polyoxyethylated nonionic surfactants and their applications in topical ocular drug delivery, *Advanced Drug Delivery Reviews* 60(15) (2008) 1663-1673.
- [7] V. Pandey, S. Kohli, Lipids and Surfactants: The Inside Story of Lipid-Based Drug Delivery Systems, 35(2) (2018) 99-155.
- [8] I. Nardin, S. Köllner, Successful development of oral SEDDS: screening of excipients from the industrial point of view, *Advanced Drug Delivery Reviews* 142 (2019) 128-140.

- [9] B. Singh, S. Bandopadhyay, R. Kapil, R. Singh, O.P. Katare, Self-Emulsifying Drug Delivery Systems (SEDDS): Formulation Development, Characterization, and Applications, 26(5) (2009) 427-451.
- [10] A. Mahmood, A. Bernkop-Schnürch, SEDDS: A game changing approach for the oral administration of hydrophilic macromolecular drugs, *Advanced Drug Delivery Reviews* 142 (2019) 91-101.
- [11] H. Hatakeyama, H. Akita, H. Harashima, The polyethyleneglycol dilemma: advantage and disadvantage of PEGylation of liposomes for systemic genes and nucleic acids delivery to tumors, *Biol Pharm Bull* 36(6) (2013) 892-9.
- [12] Q. Sun, Z. Zhou, N. Qiu, Y. Shen, Rational Design of Cancer Nanomedicine: Nanoproperty Integration and Synchronization, *Adv Mater* 29(14) (2017).
- [13] S. Giarra, N. Lupo, V. Campani, A. Carotenuto, L. Mayol, G. De Rosa, A. Bernkop-Schnürch, In vitro evaluation of tumor targeting ability of a parenteral enoxaparin-coated self-emulsifying drug delivery system, *Journal of Drug Delivery Science and Technology* 53 (2019) 101144.
- [14] A.G. Agrawal, A. Kumar, P.S. Gide, Self emulsifying drug delivery system for enhanced solubility and dissolution of glipizide, *Colloids and Surfaces B: Biointerfaces* 126 (2015) 553-560.
- [15] J.D. Friedl, C. Steinbring, S. Zaichik, N.-M.N. Le, A. Bernkop-Schnürch, Cellular uptake of self-emulsifying drug-delivery systems: polyethylene glycol versus polyglycerol surface, *Nanomedicine* 15(19) (2020) 1829-1841.
- [16] V.V. Khutoryanskiy, Beyond PEGylation: Alternative surface-modification of nanoparticles with mucus-inert biomaterials, *Advanced Drug Delivery Reviews* 124 (2018) 140-149.
- [17] C. Freese, M.I. Gibson, H.-A. Klok, R.E. Unger, C.J. Kirkpatrick, Size- and Coating-Dependent Uptake of Polymer-Coated Gold Nanoparticles in Primary Human Dermal Microvascular Endothelial Cells, *Biomacromolecules* 13(5) (2012) 1533-1543.
- [18] J. Rohrer, O. Zupančič, G. Hetényi, M. Kurpiers, A. Bernkop-Schnürch, Design and evaluation of SEDDS exhibiting high emulsifying properties, *Journal of Drug Delivery Science and Technology* 44 (2018) 366-372.

- [19] C. Schneider, O.N. Gordon, R.L. Edwards, P.B. Luis, Degradation of Curcumin: From Mechanism to Biological Implications, *J Agric Food Chem* 63(35) (2015) 7606-14.
- [20] O.N. Gordon, P.B. Luis, H.O. Sintim, C. Schneider, Unraveling curcumin degradation: autoxidation proceeds through spiroepoxide and vinyl ether intermediates en route to the main bicyclopentadione, *J Biol Chem* 290(8) (2015) 4817-4828.
- [21] R. Wibel, D.E. Braun, L. Hämmerle, A.M. Jörgensen, P. Knoll, W. Salvenmoser, C. Steinbring, A. Bernkop-Schnürch, In Vitro Investigation of Thiolated Chitosan Derivatives as Mucoadhesive Coating Materials for Solid Lipid Nanoparticles, *Biomacromolecules* 22(9) (2021) 3980-3991.
- [22] C. Leichner, C. Menzel, F. Laffleur, A. Bernkop-Schnürch, Development and in vitro characterization of a papain loaded mucolytic self-emulsifying drug delivery system (SEDDS), *International Journal of Pharmaceutics* 530(1) (2017) 346-353.
- [23] I. Pereira de Sousa, C. Steiner, M. Schmutzler, M.D. Wilcox, G.J. Veldhuis, J.P. Pearson, C.W. Huck, W. Salvenmoser, A. Bernkop-Schnürch, Mucus permeating carriers: formulation and characterization of highly densely charged nanoparticles, *European Journal of Pharmaceutics and Biopharmaceutics* 97 (2015) 273-279.
- [24] R.C. Borra, M.A. Lotufo, S.M. Gaglioti, M. Barros Fde, P.M. Andrade, A simple method to measure cell viability in proliferation and cytotoxicity assays, *Braz Oral Res* 23(3) (2009) 255-62.
- [25] V. Meunier, M. Bourrié, Y. Berger, G. Fabre, The human intestinal epithelial cell line Caco-2; pharmacological and pharmacokinetic applications, *Cell Biol Toxicol* 11(3-4) (1995) 187-94.
- [26] A. Erazo-Oliveras, N. Muthukrishnan, R. Baker, T.-Y. Wang, J.-P. Pellois, Improving the endosomal escape of cell-penetrating peptides and their cargos: strategies and challenges, *Pharmaceutics (Basel)* 5(11) (2012) 1177-1209.
- [27] B.C. Au - Evans, C.E. Au - Nelson, S.S. Au - Yu, K.R. Au - Beavers, A.J. Au - Kim, H. Au - Li, H.M. Au - Nelson, T.D. Au - Giorgio, C.L. Au - Duvall, Ex Vivo Red Blood Cell Hemolysis Assay for the Evaluation of pH-responsive Endosomolytic Agents for Cytosolic Delivery of Biomacromolecular Drugs, *JoVE* (73) (2013) e50166.

- [28] E.A. Orellana, A.L. Kasinski, Sulforhodamine B (SRB) Assay in Cell Culture to Investigate Cell Proliferation, *Bio Protoc* 6(21) (2016).
- [29] P. Foroozandeh, A.A. Aziz, Insight into Cellular Uptake and Intracellular Trafficking of Nanoparticles, *Nanoscale Research Letters* 13(1) (2018) 339.
- [30] L. Pavoni, D.R. Perinelli, A. Ciacciarelli, L. Quassinti, M. Bramucci, A. Miano, L. Casettari, M. Cespi, G. Bonacucina, G.F. Palmieri, Properties and stability of nanoemulsions: How relevant is the type of surfactant?, *Journal of Drug Delivery Science and Technology* 58 (2020) 101772.
- [31] V. Kumar, J. Qin, Y. Jiang, R.G. Duncan, B. Brigham, S. Fishman, J.K. Nair, A. Akinc, S.A. Barros, P.V. Kasperkovitz, Shielding of Lipid Nanoparticles for siRNA Delivery: Impact on Physicochemical Properties, Cytokine Induction, and Efficacy, *Molecular Therapy - Nucleic Acids* 3 (2014) e210.
- [32] N. Lupo, C. Steinbring, J.D. Friedl, B. Le-Vinh, A. Bernkop-Schnürch, Impact of bile salts and a medium chain fatty acid on the physical properties of self-emulsifying drug delivery systems, *Drug Dev Ind Pharm* 47(1) (2021) 22-35.
- [33] F. Sun, M. Adrian, N. Beztsinna, J.B. van den Dikkenberg, R.F. Maas-Bakker, P.M. van Hasselt, M.J. van Steenbergen, X. Su, L.C. Kapitein, W.E. Hennink, C.F. van Nostrum, Influence of PEGylation of Vitamin-K-Loaded Mixed Micelles on the Uptake by and Transport through Caco-2 Cells, *Mol Pharm* 15(9) (2018) 3786-3795.
- [34] A. Bernkop-Schnürch, A. Jalil, Do drug release studies from SEDDS make any sense?, *Journal of Controlled Release* 271 (2018) 55-59.
- [35] W. Seo, A.A. Kapralov, G.V. Shurin, M.R. Shurin, V.E. Kagan, A. Star, Payload drug vs. nanocarrier biodegradation by myeloperoxidase- and peroxy-nitrite-mediated oxidations: pharmacokinetic implications, *Nanoscale* 7(19) (2015) 8689-8694.
- [36] J. Griesser, G. Hetényi, H. Kadas, F. Demarne, V. Jannin, A. Bernkop-Schnürch, Self-emulsifying peptide drug delivery systems: How to make them highly mucus permeating, *International Journal of Pharmaceutics* 538(1) (2018) 159-166.
- [37] G.A. Martău, M. Mihai, D.C. Vodnar, The Use of Chitosan, Alginate, and Pectin in the Biomedical and Food Sector—Biocompatibility, Bioadhesiveness, and Biodegradability, *Polymers* 11(11) (2019) 1837.

- [38] J.D. Friedl, V. Nele, G. De Rosa, A. Bernkop-Schnürch, Bioinert, Stealth or Interactive: How Surface Chemistry of Nanocarriers Determines Their Fate In Vivo, *Advanced Functional Materials* 31(34) (2021) 2103347.
- [39] Y. De Anda-Flores, E. Carvajal-Millan, A. Campa-Mada, J. Lizardi-Mendoza, A. Rascon-Chu, J. Tanori-Cordova, A.L. Martínez-López, Polysaccharide-Based Nanoparticles for Colon-Targeted Drug Delivery Systems, *Polysaccharides* 2(3) (2021) 626-647.
- [40] S.K. Lai, Y.-Y. Wang, J. Hanes, Mucus-penetrating nanoparticles for drug and gene delivery to mucosal tissues, *Advanced Drug Delivery Reviews* 61(2) (2009) 158-171.
- [41] W. Shan, X. Zhu, M. Liu, L. Li, J. Zhong, W. Sun, Z. Zhang, Y. Huang, Overcoming the Diffusion Barrier of Mucus and Absorption Barrier of Epithelium by Self-Assembled Nanoparticles for Oral Delivery of Insulin, *ACS Nano* 9(3) (2015) 2345-2356.
- [42] M. Liu, J. Zhang, X. Zhu, W. Shan, L. Li, J. Zhong, Z. Zhang, Y. Huang, Efficient mucus permeation and tight junction opening by dissociable “mucus-inert” agent coated trimethyl chitosan nanoparticles for oral insulin delivery, *Journal of Controlled Release* 222 (2016) 67-77.
- [43] Y. Cui, W. Shan, M. Liu, L. Wu, Y. Huang, A strategy for developing effective orally-delivered nanoparticles through modulation of the surface “hydrophilicity/hydrophobicity balance”, *Journal of Materials Chemistry B* 5(6) (2017) 1302-1314.
- [44] Y.-Y. Wang, S.K. Lai, J.S. Suk, A. Pace, R. Cone, J. Hanes, Addressing the PEG Mucoadhesivity Paradox to Engineer Nanoparticles that “Slip” through the Human Mucus Barrier, *Angewandte Chemie International Edition* 47(50) (2008) 9726-9729.
- [45] H. Chen, H. Paholak, M. Ito, K. Sansanaphongpricha, W. Qian, Y. Che, D. Sun, ‘Living’ PEGylation on gold nanoparticles to optimize cancer cell uptake by controlling targeting ligand and charge densities, *Nanotechnology* 24(35) (2013) 355101.
- [46] C. He, Y. Hu, L. Yin, C. Tang, C. Yin, Effects of particle size and surface charge on cellular uptake and biodistribution of polymeric nanoparticles, *Biomaterials* 31(13) (2010) 3657-3666.
- [47] K. Sachs-Barrable, A. Thamboo, S.D. Lee, K.M. Wasan, Lipid excipients Peceol and Gelucire 44/14 decrease P-glycoprotein

mediated efflux of rhodamine 123 partially due to modifying P-glycoprotein protein expression within Caco-2 cells, *J Pharm Pharm Sci* 10(3) (2007) 319-31.

[48] C.C. Berton-Carabin, M.-H. Ropers, C. Genot, Lipid Oxidation in Oil-in-Water Emulsions: Involvement of the Interfacial Layer, *Comprehensive Reviews in Food Science and Food Safety* 13(5) (2014) 945-977.

[49] D. Wehrung, W.J. Geldenhuys, M.O. Oyewumi, Effects of gelucire content on stability, macrophage interaction and blood circulation of nanoparticles engineered from nanoemulsions, *Colloids and Surfaces B: Biointerfaces* 94 (2012) 259-265.

[50] F. Gao, Z. Zhang, H. Bu, Y. Huang, Z. Gao, J. Shen, C. Zhao, Y. Li, Nanoemulsion improves the oral absorption of candesartan cilexetil in rats: Performance and mechanism, *Journal of Controlled Release* 149(2) (2011) 168-174.

[51] J. Ye, X. Xia, W. Dong, H. Hao, L. Meng, Y. Yang, R. Wang, Y. Lyu, Y. Liu, Cellular uptake mechanism and comparative evaluation of antineoplastic effects of paclitaxel-cholesterol lipid emulsion on triple-negative and non-triple-negative breast cancer cell lines, *International journal of nanomedicine* 11 (2016) 4125-4140.

[52] S.J. Hong, M.H. Ahn, J. Sangshetti, R.B. Arote, Sugar alcohol-based polymeric gene carriers: Synthesis, properties and gene therapy applications, *Acta Biomaterialia* 97 (2019) 105-115.

[53] A. Edlich, C. Gerecke, M. Giulbudagian, F. Neumann, S. Hedtrich, M. Schäfer-Korting, N. Ma, M. Calderon, B. Kleuser, Specific uptake mechanisms of well-tolerated thermoresponsive polyglycerol-based nanogels in antigen-presenting cells of the skin, *European Journal of Pharmaceutics and Biopharmaceutics* 116 (2017) 155-163.

[54] L. Venturelli, S. Nappini, M. Bulfoni, G. Gianfranceschi, S. Dal Zilio, G. Coceano, F. Del Ben, M. Turetta, G. Scoles, L. Vaccari, D. Cesselli, D. Cojoc, Glucose is a key driver for GLUT1-mediated nanoparticles internalization in breast cancer cells, *Scientific Reports* 6(1) (2016) 21629.

[55] C. Hu, M. Niestroj, D. Yuan, S. Chang, J. Chen, Treating cancer stem cells and cancer metastasis using glucose-coated gold nanoparticles, *International journal of nanomedicine* 10 (2015) 2065-2077.

- [56] M. Moros, B. Hernáez, E. Garet, J.T. Dias, B. Sáez, V. Grazú, Á. González-Fernández, C. Alonso, J.M. de la Fuente, Monosaccharides versus PEG-Functionalized NPs: Influence in the Cellular Uptake, *ACS Nano* 6(2) (2012) 1565-1577.
- [57] Y. Fujimoto, S. Sakuma, C. Maruyama, T. Kohda, Curcumin inhibits the proliferation of a human colorectal cancer cell line Caco-2 partially by both apoptosis and G2/M cell cycle arrest, *International Journal of Pharmacological Research* 4 (2014) 84-90.
- [58] J. Lotfi-Attari, Y. Pilehvar-Soltanahmadi, M. Dadashpour, S. Alipour, R. Farajzadeh, S. Javidfar, N. Zarghami, Co-Delivery of Curcumin and Chrysin by Polymeric Nanoparticles Inhibit Synergistically Growth and hTERT Gene Expression in Human Colorectal Cancer Cells, *Nutr Cancer* 69(8) (2017) 1290-1299.
- [59] T. Lund, M.F. Callaghan, P. Williams, M. Turmaine, C. Bachmann, T. Rademacher, I.M. Roitt, R. Bayford, The influence of ligand organization on the rate of uptake of gold nanoparticles by colorectal cancer cells, *Biomaterials* 32(36) (2011) 9776-9784.

Author CRediT Statement:

Julian D. Friedl: Conceptualization, Methodology, Investigation, Writing - Original Draft; Visualization, Writing - Review & Editing

Arne Matteo Jörgensen: Methodology, Writing - Review & Editing

Nguyet-Minh Nguyen Le: Methodology, Writing - Review & Editing

Christian Steinbring: Methodology, Investigation, Visualization, Writing - Original Draft

Andreas Bernkop-Schnürch: Conceptualization, Writing - Review & Editing, Supervision, Funding acquisition

Declaration of interests

The authors declare that they have no known competing financial interests or personal relationships that could have appeared to influence the work reported in this paper.

The authors declare the following financial interests/personal relationships which may be considered as potential competing interests:

Julian Friedl reports financial support was provided by doctoral scholarship for the promotion of young researchers at the Leopold-Franzens-University Innsbruck. Nguyet-Minh Nguyen Le reports financial support was provided by doctoral scholarship for the promotion of young researchers at the Leopold-Franzens-University Innsbruck.

Highlights

- Polyethylene glycol- (PEG-) surfactants in self-emulsifying drug delivery system (SEDDS) can be successfully substituted by surfactants bearing polyhydroxy head groups
- Mucus permeation of SEDDS with polyhydroxy-decorated surfaces was comparable to conventional SEDDS with PEGylated surface
- Long PEG-chains on SEDDS surfaces were identified to impair cellular uptake and increase endosomal and lysosomal entrapment
- Polyhydroxy-decorated surfaces on SEDDS promoted superior cellular internalisation and showed only negligible co-localisation with lysosomes
- Polyhydroxy-decorated SEDDS surfaces outperformed conventional PEGylated SEDDS surfaces in inhibiting tumor cell proliferation after cytosolic delivery of curcumin
-